Journal of Power Sources 196 (2011) 1324–1328

Contents lists available at ScienceDirect

Journal of Power Sources

journal homepage: www.elsevier.com/locate/jpowsour

Short communication

Carbon supported ruthenium chalcogenide as cathode catalyst in a microfluidic formic acid fuel cell

A.S. Gago [a], D. Morales-Acosta [b], L.G. Arriaga [b], N. Alonso-Vante [a,*]

[a] Laboratory of Electrocatalysis, UMR-CNRS 6503, Université de Poitiers, 40 Avenue du Recteur Pineau, F-86022 Potiers Cedex, France
[b] Centro de Investigación y Desarrollo Tecnológico en Electroquímica, S.C. Parque Tecnológico Querétaro Sanfandila, P.O. Box 064, Pedro Escobedo, 76703, Querétaro, Mexico

ARTICLE INFO

Article history:
Received 30 June 2010
Received in revised form 17 August 2010
Accepted 30 August 2010
Available online 8 September 2010

Keywords:
Ruthenium chalcogenide catalyst
Microfluidic fuel cell
Fuel cross-over
Ru_xSe_y/C
Pt/C

ABSTRACT

This work reports the electrochemical measurements of 20 wt.% Ru_xSe_y/C for oxygen reduction reaction (ORR) in presence of different concentration of HCOOH and its use as cathode catalyst in a microfluidic formic acid fuel cell (μFAFC). The results were compared to those obtained with commercial Pt/C. Half-cell electrochemical measurements showed that the chalcogenide catalyst has a high tolerance and selectivity towards ORR in electrolytes containing up to 0.1 M HCOOH. The depolarization effect was higher on Pt/C than on Ru_xSe_y/C by a factor of ca. 23. Both catalysts were evaluated as cathode of a μFAFC operating with different concentrations of HCOOH. When 0.5 M HCOOH was used, maximum current densities of 11.44 mA cm^{-2} and 4.44 mA cm^{-2} were obtained when the cathode was Ru_xSe_y/C and Pt/C, respectively. At 0.5 M HCOOH, the peak power density of the μFAFC was similar for both catalysts, ca. 1.9 mW cm^{-2}. At 5 M HCOOH the power density of the μFAFC using Ru_xSe_y, was 9.3 times higher than the obtained with Pt/C.

1. Introduction

Direct methanol fuel cells (DMFCs) are one of the most attractive energy generators systems for portable electronics (i.e. cell phones, smart phones, tablet computers and laptops) because of their ease, safe handling, distribution, storage of the fuel, and high-energy density [1–3]. Nonetheless the commercialization of DMFCs is still hindered by a number of problems such as fuel cross-over, water management, etc. [2,4–6]. One alternative to DMFCs for powering portable devices is microfluidic formic acid fuel cells (μFAFCs) [7–10]. Since no turbulent mixing exists at the microscale, the laminar flow regime permits to two streams to be carried in a single micro-channel. This laminar property of the two flows eliminates the need for a membrane, while still allowing for ionic transport between the anode and the cathode [11–13]. The problem of fuel cross-over always occurs for this kind of cells, but it can be minimized by adjusting cell dimensions and stream flow rates [7,9] or using a nanoporous membrane [14,15]. Nevertheless the device complexity increases requiring more sophisticate ancillary systems and therefore the cost of the system becomes higher. One approach to overcome this problem is to use tolerant catalysts as cathodes in microfluidic fuel cells [12,16]. This class of catalyst in this kind of cell not only has a direct positive impact in the performance of the cell, using a fuel like formic acid, but also in the design of the cell by itself. Summarizing, the advantages of using a formic acid tolerant cathode catalyst are: (i) the increment of the output power density using high concentrated formic acid as fuel [16], (ii) the reduction in the separation between the electrodes, thus making the μFAFC smaller. This is an absolute requirement if the cell is intended for powering portable electronic devices [1], (iii) fuel cross-over is not anymore an issue, therefore nanoporous membranes or separators to reduce the fuel cross-over the fluids are not needed [14,15], (iv) longer channels in the cell can be elaborated, increasing the exposed active area of the cathode, increasing the power density, (v) the reduction of the flow speed of the inlet fluids, therefore less power for the micro-pumps is required [17], and (vi) high concentrations of HCOOH can be used, thus increasing the stored energy density per volume that can be carried in portable devices [18]. It is worth noting that already commercial DMFCs such as Toshiba Dynaro and MTI Micro's DMFC with Mobion chip technology utilize high purity fuel (> 99%) [19–21].

Cluster-like compounds such as Ru_xSe_y have proven to be highly tolerant and selective to oxygen reduction reaction in presence of methanol molecules [22–27]. Herein we report the electrochemical results of ORR measurements of Ru_xSe_y in different HCOOH concentrations catalyst as well as its evaluation in a μFAFC. The results were compared to those obtained with commercial Pt/C catalyst in the same conditions.

* Corresponding author. Tel.: +33 54945 3625; fax: +33 54945 3580.
E-mail address: nicolas.alonso.vante@univ-poitiers.fr (N. Alonso-Vante).

0378-7753/$ – see front matter © 2010 Elsevier B.V. All rights reserved.
doi:10.1016/j.jpowsour.2010.08.109

2. Experimental

2.1. Synthesis of Ru_xSe_y/C catalyst

Carbon supported Ru_xSe_y catalyst (20 wt.%) was synthesized as reported elsewhere [28,29]. $RuCl_3{\cdot}xH_2O$ and SeO_2 were used as chemical precursors. Typically, 0.124 g Vulcan XC-72 carbon was dispersed in 100 mL of water under nitrogen and vigorous stirring by a bar magnet (400 rpm) and the resulting suspension was heated to 80 °C, mixed at this temperature for 30 min to remove oxygen in water, and then cooled down to room temperature. Subsequently, 4 mmol $RuCl_3$ (83 mg) and 1 mmol SeO_2 (11 mg) were added to the above suspension and then stirred for 1 h. Thereafter, 100 mL of a mixture solution containing 0.1 M $NaBH_4$ and 0.2 M NaOH was added drop wise to the suspension to reduce Ru^{3+} and Se^{4+} to Ru^0 and Se^0, respectively. After complete addition of the reducing solution, the suspension was kept for further reaction another 10 min and then heated to 80 °C for 10 min to enhance the chemical reaction. The final black powder was collected on a Millipore filter membrane (0.22 μm, pore size dia.), washed with distilled water, and dried under vacuum at room temperature.

2.2. Electrode preparation and electrochemical measurements

Ru_xSe_y/C ink was prepared by dispersing 10 mg catalyst powder in 250 μL Nafion® (5 wt.% in water/aliphatic alcohols solution, Aldrich) and 1250 μL ultra pure water in an ultrasound bath for 1 h. The same procedure was followed for the preparation of the ink of 20 wt.% Pt/C E-TEK. Aliquots of 5 μL of the electrocatalytic inks were deposited onto glassy carbon disks previously polished with Al_2O_3 powder (5A) until a mirror finished surface (3 mm dia.). The prepared electrodes were dried under a nitrogen flow. This procedure produced homogeneous films as observed by the optical microscope.

Rotating disk electrodes (RDE), and linear voltammetry measurements were done in one-compartment electrochemical cell. The temperature was kept constant at 25 °C. A glassy carbon plate (1 cm^2) served as the counter electrode. Electrode potential was measured via a reference hydrogen electrode (RHE) connected to the cell with a Luggin capillary. The working electrodes were deposited on glassy carbon. All electrolytes were prepared with Milli-Q water (18 MΩ cm). The base electrolyte was 0.5 M H_2SO_4 (97.9%, J.T. Baker). The measurements were performed, first in the base electrolyte and varying concentrations of formic acid (88%, Fermont), i.e. 0.01 M, 0.1 M, 1 M and 5 M. Current-potential curves were recorded with a potentiostat (μAutolab type III).

2.3. Microfluidic fuel cell fabrication and catalyst deposition

Cell construction method has been reported previously [30]. The μFAFC employed in this study was made of PMMA, whose dimensions are 2 mm width (each channel 1 mm), 1 mm high and 45 mm long with an electrode area of 0.45 cm^2. Anode and cathode catalysts were deposited on the walls of graphite electrodes by spray technique. The ink prepared previously from a mixture of Nafion®-isopropanol and powders of the electrocatalyst materials was sprayed. Two micro fuel cells were constructed in order to compare 20 wt.% Ru_xSe_y/C and 30 wt.% Pt/C (E-TEK) as cathode catalysts with the same loading catalyst: 1.1 mg cm^{-2}. As anode catalyst 20 wt.% Pd/C (E-TEK) was maintained in both cells with a loading of 1.1 mg cm^{-2} and 1.7 mg cm^{-2}, respectively.

2.4. Microfluidic formic acid fuel cell tests

Several formic acid concentrations (0.1 M, 0.5 M, 1 M and 5 M) in 0.5 M H_2SO_4 were used as the fuel and oxygen (4.3 U.A.P. Praxair) as oxidant dissolved in 0.5 M H_2SO_4. An increment in the saturation of oxidant in sulfuric acid media was done by humidification of the oxygen gas with a saturation tower [30].

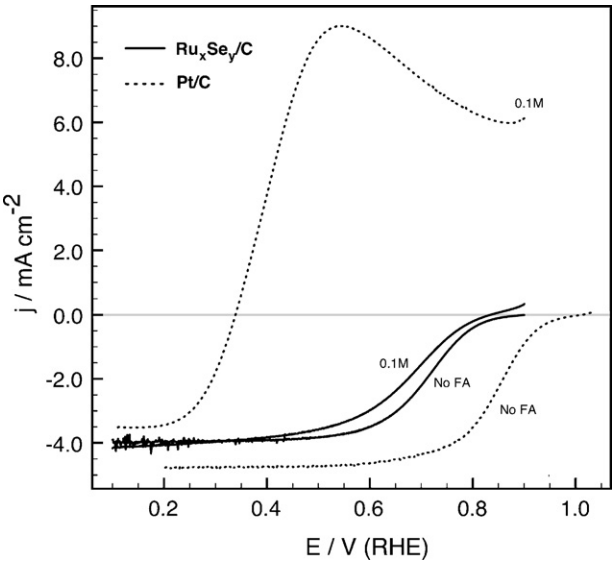

Fig. 1. ORR curves for Ru_xSe_y/C (continuous line) and 20 wt.% Pt/C E-TEK (dotted line) in O_2-purged xHCOOH + 0.5 M H_2SO_4 (x = 0 and 0.1). "No FA" legend corresponds to 0 M. Measurements were carried out at 5 mV s^{-1}, at the rotation of 1600 rpm.

In all the fuel cell experiments, the cathode (O_2-purged H_2SO_4) and anode (HCOOH–H_2SO_4) flow rates were kept on 1.2 mL min^{-1} and 0.1 mL min^{-1}, respectively. Fluid flow in all fuel cell experiments was pressure driven using a peristaltic pump (Masterflex Cole-Palmer Mod-7553-70). This flow rate and the cell dimensions correspond to a Reynolds number 0.1, assuring the laminar flow range. Voltage and current measurements were performed utilizing a potentiostat/galvanostat (Autolab PGSTAT30). All tests were performed at room temperature.

3. Results and discussion

3.1. Oxygen reduction reaction in presence of HCOOH

Fig. 1 shows typical ORR curves (1600 rpm) of 20 wt.% Pt/C and 20 wt.% Ru_xSe_y/C in the presence of molecular oxygen in 0.5 M H_2SO_4. In 0.1 M HCOOH (FA) electrolyte the Pt/C showed a large anodic current peaking at 0.54 V *vs.* RHE because of the oxidation of formic acid on Pt/C catalyst. Under this condition, the non-tolerance of Pt produces a shift of the onset potential for the ORR of ca. −660 mV. This result is attributed to the formation of a mixed-potential, which is caused by the simultaneous oxidation of HCOOH and ORR on Pt/C catalyst. For Ru_xSe_y/C the onset potential for ORR in 0.1 M HCOOH + 0.5 M H_2SO_4 was only shifted by ca. −45 mV. It was, thus, clear that the Ru_xSe_y/C catalyst remained highly selective towards ORR in formic acid containing electrolyte, in other words more tolerant than Pt/C, making it potentially a more active cathode catalyst for its application in a μFAFC. Another consequence of the difference in the selectivity is that it gives rise to a small variation of the diffusion limiting current, as observed for platinum. Further RDE analysis as a function of the formic acid concentration is depicted in Tafel plot in Fig. 2 after ORR mass-transfer correction for 20 wt.% Pt/C and Ru_xSe_y/C. Here it is clearly observed the influence of the formic acid concentration on both catalysts as well as the degree of selectivity on the chalcogenide. This can be read at a defined current density, e.g., $|j|$ = 0.2 mA cm^{-2}. A minimum FA concentration (0.1 M) is sufficient to depolarize Pt/C by −615 mV

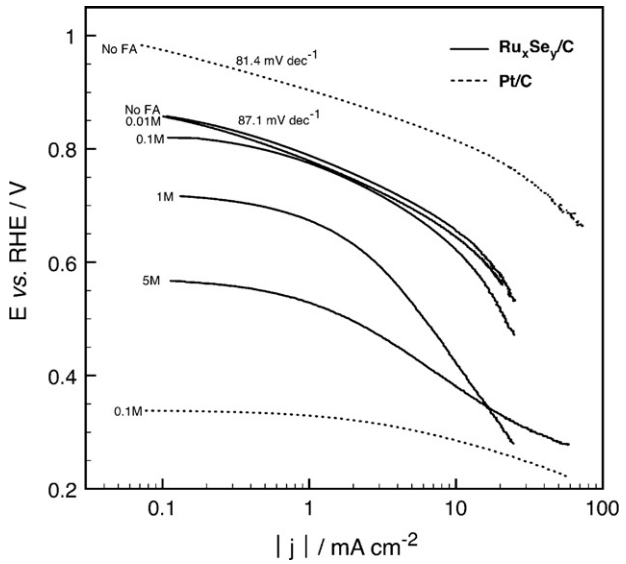

Fig. 2. ORR corrected mass-transfer Tafel plots for 20 wt.% Ru_xSe_y/C (continuous line) in O_2-purged 0.5 M H_2SO_4 + x M HCOOH (x = 0, 0.01, 0.1, 1, 5) electrolyte at 25 °C. "No FA" legend corresponds to 0 M. Catalyst 20 wt.% Pt/C E-TEK (dashed line) is also indicated for 0 and 0.1 M HCOOH.

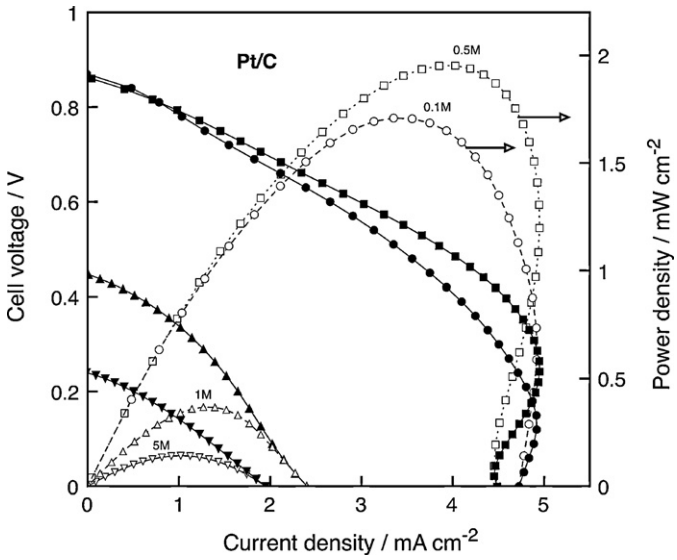

Fig. 4. Polarization and power density curves for 30 wt.% Pt/C E-TEK (1.1 mg cm^{-2}) in the μFAFC operating with 0.1 (●), 0.5 (■), 1 (▲) and 5 M (▼), T = 25 °C, Flow rate = 1.2 mL min^{-1}. 20 wt.% Pd/C E-TEK (1.7 mg cm^{-2}) was used as anode catalyst.

in comparison to Ru_xSe_y/C which is depolarized by −27 mV. Therefore the depolarization effect on Pt/C is ca. 23 times higher than on Ru_xSe_y/C. Although Ru_xSe_y/C keeps a higher selectivity than Pt/C at higher concentration, the depolarization effect becomes more evident and at 5 M this depolarization attains −280 mV. Another interesting feature on the chalcogenide to be observed is the average Tafel slope of 85.9 mV dec^{-1}. This latter is similar to that of Pt/C (81.4 mV dec^{-1}) meaning that the kinetics for ORR is not perturbed by the presence of adsorbed HCOOH. It is not possible to distinguish a Tafel slope for 1 M and 5 M HCOOH which stress the fact that for this concentration the reaction mechanism is not governed solely by the ORR [31].

Selected Koutecky–Levich plots for the ORR, in absence and presence of formic acid, on Ru_xSe_y/C and Pt/C are summarized in Fig. 3 at an applied electrode potential of 0.2 V/RHE. A series of straight lines was obtained for both systems, and apparently dependent on the formic acid concentration, as observed for the chalcogenide electrode. The Koutecky–Levich equation: $j^{-1} = j_k{}^{-1} + j_d{}^{-1}$, where j_k and $j_d = B\omega^{1/2}$ correspond to the kinetic and diffusion currents, fits all straight lines. The theoretical slope, $1/B$, for n = 4 electrons (in free formic acid solution), calculated from $B = 0.63nFAC * D_{O_2}^{2/3}\nu^{-1/6} = 0.32$ mA cm^{-2} rpm$^{-1/2}$, is indicated as dotted line in the figure. This slope was obtained using a bulk O_2 solubility, diffusion coefficient, and kinematic viscosity of 1.1×10^{-6} mol cm^{-3}, 1.40×10^{-5} cm^2 s^{-1} and 0.01 cm^2 s^{-1} in H_2SO_4 solution, respectively. The calculated slope contrasted by the experimental one (0.4 mA cm^{-2} rpm$^{-1/2}$) for the chalcogenide electrode confirms that ORR charge transfer reaction is being mostly performed via the 4 electrons pathway. On both electrodes the effect of formic acid is reflected by an increase of $1/B$ slope. Using formic acid from 0.1 M to 5 M produces an increase of ca. 13% of the slope. Within this formic acid concentration interval the electrolyte kinematic viscosity is also influenced [32]. According to the Stokes–Einstein equation, for diffusion of spherical particles through liquid with a low Reynolds number, the change in the kinematic viscosity contributes to a slope variation of ca. 11%. Therefore, the observed change in the slope can be mainly attributed to the viscosity and bulk oxygen concentration variation.

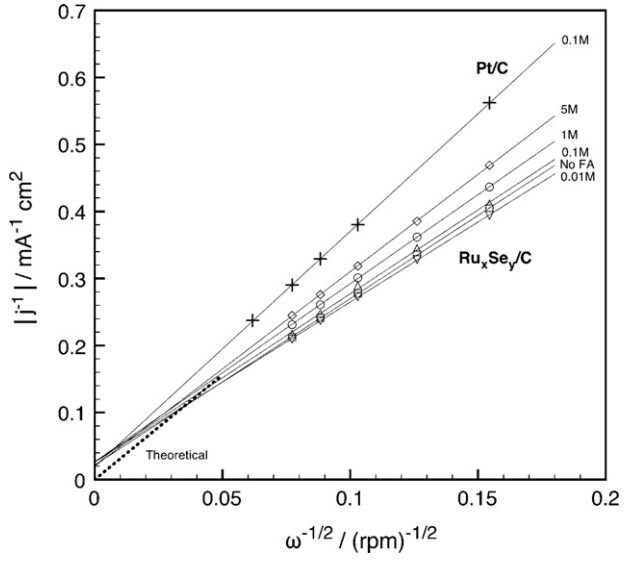

Fig. 3. Koutecky–Levich plots determined from ORR for Ru_xSe_y/C electrocatalyst in O_2-purged 0.5 M H_2SO_4 + x M HCOOH with x = (□) 0, (▽) 0.01, (△) 0.1, (○) 1, and (◊) 5 M at 0.2 V *vs.* RHE. Pt/C in 0.5 M O_2-purged H_2SO_4 + 0.1 M HCOOH is also shown as + symbol. The dotted line refers to the theoretical calculated slope for n = 4 electrons.

3.2. Microfluidic fuel cell measurements using HCOOH as fuel

The fuel cell polarization and power density at several formic acid concentrations for commercial Pt/C cathode are shown in Fig. 4. At a formic acid concentration of 0.1 M the potential of the cell drops at higher current densities attaining a plateau at ca. 4.5 mA cm^{-2}. This phenomenon is certainly due to mass transport limitations. Consequently the performance of the cell is low achieving only a peak power density of 1.71 mW cm^{-2} (see Table 1). When the formic acid concentration is increased to 0.5 M the cell shows a maximum performance achieving a current and power density of 4.44 mA cm^{-2} and 1.97 mW cm^{-2}, respectively. Since both fluids are kept separately the effect from HCOOH cross-over is not yet evident as in half-cell measurements. At high concentrations (1 M and 5 M) the performance of the cell drops dramatically. The electromotive force (E_{emf}) of the cell decreases from 0.86 V for 0.1 M HCOOH to 0.46 V and 0.24 V for 1 M and 5 M, respectively.

Table 1
Peak power density and current density of the μFAFC for both cathode configurations.

HCOOH (M)	Pt/C			Ru_xSe/C		
	E_{emf} (V)	j_{max} (mA cm^{-2})	W_{max} (mW cm^{-2})	E_{emf} (V)	j_{max} (mA cm^{-2})	W_{max} (mW cm^{-2})
0.1	0.87	4.73	1.71	0.77	7.73	1.43
0.5	0.86	4.44	1.97	0.84	11.44	1.89
1	0.46	2.40	1.31	0.75	10.89	1.76
5	0.24	1.95	0.14	0.71	7.73	1.30

This clearly indicates the cross-over effect leading to the formation of a mixed-potential at the cathode, i.e. formic acid oxidation and oxygen reduction reaction. The formic acid molecules diffuse from anolyte to catholyte trough the mixing region. The width of the diffusive mixing region can be calculated using the following expression [12]: $\Delta x \approx (Dhy/U)^{1/3}$, where h is the channel height, y the distance the fluid flows down-stream, and U the average flow speed. For the particular geometry of the cell used at a down-stream position of 4 mm (0.5 mm from the outlet), $\Delta x \approx 0.13$ mm, assuming a diffusion coefficient of $D = 5 \times 10^{-6}$ cm^2 s^{-1}. Moreover, a simulation study using FEMLAB has shown that at a flow rate of 1:1 (anolyte and catholyte) fuel cross-over is quite evident [7]. The concentration of HCOOH close to the cathode, near the end of a channel of 2.5 mm long, is ~0.15 M. This value increases as the channel becomes longer and as the concentration of the fuel is higher. While this effect can be reduced increasing flow rate of cathode stream, as it was done for this work, fuel cross-over is still present. The lack of selectivity of ORR on Pt in the presence of HCOOH, cause the mixed-potential and therefore the E_{emf} of the cell drops. Another reason for the low performance of the cell at higher concentrations of HCOOH is the decrease of the solution conductivity. Indeed, preliminary conductivity measurements of 1 M, 5 M and 10 M HCOOH in 0.5 M H_2SO_4 were 191.1 mS cm^{-1}; 128.8 mS cm^{-1}; and 75.9 mS cm^{-1}, respectively. A further analysis of all the factors above mentioned should be taken into account to optimize cell performance.

Fig. 5 shows the results of equivalent fuel cell tests using Ru_xSe_y/C cathode configuration in several formic acid concentrations (0.1 M, 0.5 M, 1 M and 5 M). The μFAFC reaches its maximum power density when using 0.5 M HCOOH as fuel. This value is only 0.08 mW cm^{-2} lower than the one achieved with Pt/C at the same formic concentration, but the maximum measured current density was 2.6 times higher than Pt/C, see Table 1. The reason of this is because the mass transport limitations were not present for Ru_xSe_y/C as for Pt/C. It is worth to note that for all formic acid concentrations the μFAFC with Ru_xSe_y/C catalyst gave higher maximum current densities than Pt. However, the true advantage of using the tolerant catalyst instead of Pt/C is not yet evident. At concentrations of 1 M and 5 M the power density of the cell, using Ru_xSe_y/C as cathode, drops to 1.76 mW cm^{-2} and 1.30 mW cm^{-2}, respectively. Compared to the power achieved with 0.5 M HCOOH this drop is only 7% and 30% for 1 M and 5 M HCOOH, respectively, compared to a drop of 34% and 93% for Pt/C. While the same phenomenon of fuel cross-over exists, its negative effect on the cell using the chalcogenide catalyst is less predominant than with Pt/C. At a concentration of 5 M the power density of the μFAFC with Ru_xSe_y/C is 9.3 times higher than Pt/C. These facts are in good agreement with results obtained in half-cell experiments, and a clear and direct consequence of the high tolerance and selectivity of the chalcogenide catalyst. Compared to Pt/C, the mixed-potential of Ru_xSe_y/C is more positive and therefore a smaller shift in the E_{emf}, cf. Fig. 2. The E_{emf}, the current and maximum power density values for both configuration cells with different cathode catalysts and at each of formic acid concentrations are shown in Table 1.

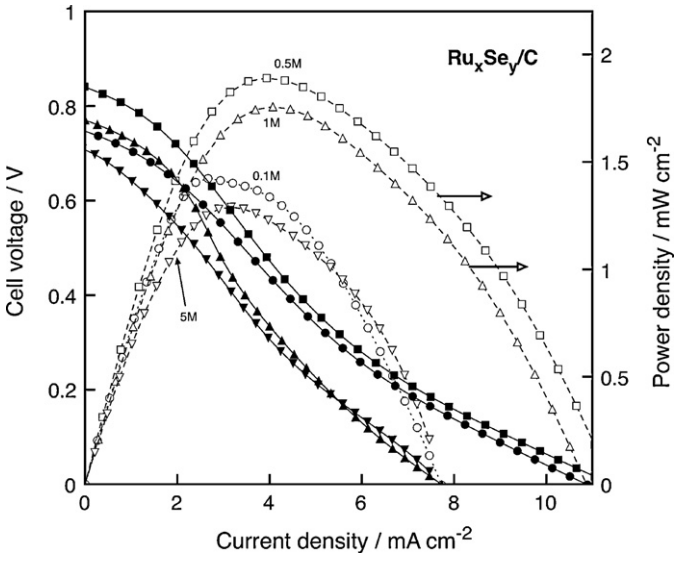

Fig. 5. Polarization and power density curves for 20 wt.% Ru_xSe_y/C (1.1 mg cm^{-2}) in the μFAFC operating with 0.1 (●), 0.5 (■), 1 (▲) and 5 M (▼), $T = 25$ °C, flow rate = 1.2 mL min^{-1}. $T = 25$ °C, flow rate = 1.2 mL min^{-1}. 20 wt.% Pd/C E-TEK (1.7 mg cm^{-2}) was used as anode catalyst.

4. Conclusions

The high tolerance and selectivity of 20 wt.% Ru_xSe_y/C catalyst has been put in evidence in this work trough electrochemical experiments and its corresponding microfluidic formic acid fuel cell tests. The kinetics for the ORR by the chalcogenide catalyst is not perturbed in electrolytes containing up to 0.1 M HCOOH. At 0.1 mA cm^{-2} it showed a significant smaller depolarization effect than the commercial catalyst (20 wt.% Pt/C). As cathode catalyst in the μFAFC, Ru_xSe_y/C had a similar performance than Pt/C when 0.5 M HCOOH was used as fuel. However, when 5 M HCOOH was fed to the cell with the chalcogenide catalyst, it achieved a power density 9.3 higher than when using Pt/C catalyst. Additionally, when the cell was polarized close to 0 V it produced higher current densities with Ru_xSe_y/C catalyst than Pt/C, for all HCOOH concentrations. The results obtained from the half-cell electrochemical measurements agree well with the ones obtained with the μFAFC. They clearly demonstrate that a formic acid tolerant catalyst is more suitable than platinum to be used as cathode of a micro fluidic formic acid fuel cell.

Acknowledgments

The authors gratefully acknowledge financial support from the Mexican Council for Science and Technology (CONACyT, Grant 61067 and 305477), and A.S. Gago thanks CONACYT for the scholarship.

References

[1] A. Kundu, J. Jang, J. Gil, C. Jung, H. Lee, S. Kim, B. Ku, Y. Oh, J. Power Sources 170 (2007) 67–78.

[2] S.K. Kamarudin, F. Achmad, W.R.W. Daud, Int. J. Hydrogen Energy 34 (2009) 6902–6916.
[3] C. Stone, Fuel Cells Bull. 2007 (2007) 12–15.
[4] G. Apanel, E. Johnson, Fuel Cells Bull. 2004 (2004) 12–17.
[5] R. Szweda, III-Vs Review Adv. Semicon. Mag. 19 (2006) 48.
[6] V.P. Mcconnell, Fuel Cells Bull. 2009 (2009) 12–16.
[7] R.S. Jayashree, S.K. Yoon, F.R. Brushett, P.O. Lopez-Montesinos, D. Natarajan, L.J. Markoski, P.J.A. Kenis, J. Power Sources (2010) 1–10.
[8] R.S. Jayashree, L. Gancs, E.R. Choban, A. Primak, D. Natarajan, L.J. Markoski, P.J.A. Kenis, J. Am. Chem. Soc. 127 (2005) 16758–16759.
[9] A. Bazylak, D. Sinton, N. Djilali, J. Power Sources 143 (2005) 57–66.
[10] E.R. Choban, L.J. Markoski, A. Wieckowski, P.J.A. Kenis, J. Power Sources 128 (2004) 54–60.
[11] E. Kjeang, R. Michel, D. Harrington, N. Djilali, D. Sinton, J. Am. Chem. Soc. 130 (2008) 4000–4006.
[12] E. Kjeang, N. Djilali, D. Sinton, J. Power Sources 186 (2009) 353–369.
[13] R. Jayashree, M. Mitchell, D. Natarajan, L. Markoski, P.J.A. Kenis, Langmuir 23 (2007) 6871–6874.
[14] A. Hollinger, R. Maloney, L. Markoski, P.J.A. Kenis, 214th ECS Meeting, The Electrochemical Society, 2008 (Abstract #701).
[15] A.S. Hollinger, R.J. Maloney, R.S. Jayashree, D. Natarajan, L.J. Markoski, P.J.A. Kenis, J. Power Sources (2010) 1–6.
[16] D. Whipple, R. Jayashree, D. Egas, N. Alonso-Vante, P.J.A. Kenis, Electrochim. Acta 54 (2009) 4384–4388.
[17] E. Choban, L. Markoski, A. Wieckowski, P.J.A. Kenis, J. Power Sources 128 (2004) 54–60.
[18] T.S. Zhao, W.W. Yang, R. Chen, Q.X. Wu, J. Power Sources 195 (2010) 3451–3462.
[19] Fuel Cells Bulletin 2009 (2009) 6–7.
[20] Fuel Cells Bulletin 2009 (2009) 6–6.
[21] Fuel Cells Bulletin 2009 (2009) 7–7.
[22] L. Colmenares, Z. Jusys, R. Behm, J. Phys. Chem. C 111 (2007) 1273–1283.
[23] K. Wippermann, B. Richter, K. Klafki, J. Mergel, G. Zehl, I. Dorbandt, P. Bogdanoff, S. Fiechter, S. Kaytakoglu, J. Appl. Electrochem. 37 (2007) 1399–1411.
[24] M. Montiel, S. García, P. Hernández-Fernández, R. Díaz, S. Rojas, J.L.G. Fierro, E. Fatás, P. Ocón, J. Power Sources (2009).
[25] H. Cheng, W. Yuan, K. Scott, Fuel Cells 7 (2007) 16–20.
[26] H. Cheng, W. Yuan, K. Scott, D. Browning, J. Lakeman, Appl. Catal. B. Environ. 75 (2007) 221–228.
[27] H. Cheng, W. Yuan, K. Scott, D. Browning, J. Lakeman, J. Power Sources 172 (2007) 597–603.
[28] S.A. Campbell, US Patent 2004/00967284A.
[29] C. Delacôte, A. Bonakdarpour, C. Johnston, P. Zelenay, A. Wieckowski, Faraday Discuss. 140 (2009) 269–281.
[30] D. Morales-Acosta, H. Rodríguez, G.L.A. Godinez, L.G. Arriaga, J. Power Sources 195 (2010) 1862–1865.
[31] A.S. Gago, L.G. Arriaga, Y. Gochi-Ponce, Y.J. Feng, N. Alonso-Vante, J. Electroanal. Chem. 648 (2010) 78–84.
[32] D.R. Lide (Ed.), Handbook of Chemistry and Physics, vol. 84, CRC Press, 2003.